Detecting changes in serial myocardial perfusion SPECT: A simulation study

Tracy L. Faber, PhD, Jan Modersitzki, PhD, Russell D. Folks, BS, CNMT, and Ernest V. Garcia, PhD

Background. **New algorithms were evaluated for their efficacy in detecting and quantifying serial changes in myocardial perfusion from single photon emission computed tomography (SPECT).**

Methods and Results. **We generated 72 simulations with various left ventricular positions, sizes, count rates, and perfusion defect severities using the nonuniform rational B-splines (NURBs)-based CArdiac Torso (NCAT) phantom. Images were automatically aligned by use of both full linear and rigid transformations and quantified for perfusion by use of the CEqual program. Changes within a given perfusion defect were compared by use of a Student *t* test before and after registration. Registration approaches were compared by use of receiver operating characteristic analysis. Changes of 5% were not detected well in single patients with or without alignment. Changes of 10% and 15% could be detected with false-positive rates of 15% and 10%, respectively, in single studies if alignment was performed before perfusion analysis. Alignment also reduced the number of studies necessary to demonstrate a significant perfusion change ($P < .05$) in groups of patients by about half.**

Conclusion. **Comparison of mean uptake by *t* values in SPECT perfusion defects can be used to detect 10% and greater differences in serial perfusion studies of single patients. Image alignment is necessary to optimize automatic detection of perfusion changes in both single patients and groups of patients. (J Nucl Cardiol 2005;12:302-10.)**

Key Words: Single photon emission computed tomography • *t* values • myocardial perfusion

Comparisons of visual and quantitative results between serial perfusion scans are being used increasingly to assess significant changes resulting from surgical interventions, drug therapies, and lifestyle modifications. For example, "before-and-after" perfusion scans have been used to evaluate gene therapy as a treatment for myocardial ischemia,[1] to study the effects of verapamil on heart failure patients,[2] and to investigate long-term effects of angioplasty on diabetic patients.[3] Groups of patients are often evaluated with serial imaging to compare various treatment approaches. For example, changes in perfusion over time have been used to compare the long-term effects of revascularization versus medical therapies.[4,5] Serial studies have even been used to investigate the effects of other therapies on the heart, such as irradiation for lung cancer or right ventricular pacing.[6,7] As new devices, new medicines, and new interventions are developed, accurate evaluation of their effects becomes very important, in view of maximizing patient benefit while maintaining economic efficiency. Improved methods for detecting changes will reduce the sample size, or number of test subjects, needed to reach statistical significance when evaluating new therapies or comparing different treatments and should generally accelerate clinical trials while decreasing their costs. Better methods for detecting perfusion differences will allow quicker and more accurate identification of an effective therapy for a single patient, reduce the use of ineffective treatments, more quickly indicate the necessity of an intervention, and ideally speed recovery.

It is widely recognized that computer quantification of myocardial perfusion images improves not only overall diagnostic accuracy but also enhances reliability, confidence, and reproducibility of interpretation.[8] These nuclear imaging quantitative approaches are well established for assessing abnormalities in myocardial perfu-

From the Department of Radiology, Emory University, Atlanta, Ga. Dr Modersitzki is currently affiliated with the Department of Mathematics, University of Luebeck, Luebeck, Germany.

This research was funded in part by NIH HL068904.

Received for publication Sept 10, 2004; final revision accepted Dec 20, 2004.

Reprint requests: Tracy L Faber, PhD, Division of Nuclear Medicine, Emory University Hospital, 1364 Clifton Road, NE, Atlanta, GA 30322; *Tracy_Faber@emory.org.*

1071-3581/$30.00

doi:10.1016/j.nuclcard.2004.12.299

sion and/or metabolism, usually by comparison to a normal database or by use of visual interpretation to an expected normal pattern.[9,10] However, these approaches have not been developed to quantify changes between studies, such as would be needed to assess the effects of interventions, medical therapy, or the progression or regression of coronary artery disease. The goal of this study was to investigate new quantitative algorithms for their efficacy in detecting and quantifying serial changes in myocardial perfusion from single photon emission computed tomography (SPECT). Optimal automatic detection of changes in serial SPECT studies requires alignment of the left ventricles in both images and mathematical comparison of perfusion distributions. This report describes and evaluates techniques for performing both of these operations. Because of the difficulty in determining the true changes in clinical studies, we used the NURBs-based CArdiac Torso (NCAT) software phantom to simulate realistic SPECT images in which the perfusion defects were completely characterized and actual differences in perfusion were known.

METHODS

Simulations

To generate test data, we used the 4-dimensional NCAT phantom from the University of North Carolina.[11,12] This phantom includes a model of the heart with many options for varying the simulation, including addition of cardiac and respiratory motions, inclusion of perfusion abnormalities, variations in radioactivity concentration in noncardiac structures, and creation of differing numbers of output gates. We included our own enhancement to this phantom, which allows for the use of left ventricular (LV) boundaries and perfusion defect size and location obtained from actual SPECT perfusion studies.[13] The NCAT phantom software creates gold-standard activity and attenuation maps. In this study we used the NCAT to create activity and attenuation maps for 8 frames in the cardiac cycle, in addition to average, "ungated" activity and attenuation maps. Further analysis was performed only on the ungated activity and attenuation maps.

We used 3 different LV models, obtained from 3 different actual SPECT perfusion studies. For each of the 3 models, a single perfusion defect was included in 1 of the 3 main coronary artery territories. Thus one model had an anterior defect, the second had a lateral defect, and the third had an inferior defect. The size of each simulated defect was based on the size of the actual defect in the original patient study, and these values were 20%, 30%, and 40% of total LV myocardial volume.

For each of the three models, we generated 6 simulations, one each with a defect severity of either 50%, 55%, 60%, 65%, 70%, or 75% of maximum LV perfusion. Each of these 6 perfusion defect severities was used 4 times with the same LV model to yield a total of 24 simulations per model. For all simulations, we allowed the position and orientation of the left ventricle within the chest, the LV size, the "normal" LV count value, and the count rates in adjacent organs to vary randomly about a central value. In 12 of 24 simulations, we limited LV size changes to less than 10%, where size in this case indicates a global scaling of the entire heart, for all frames in the cardiac cycle. We allowed the LV size to change by more than 10% in the second set of 12. This was to evaluate more closely the alignment algorithm that would provide more accurate results for smaller and larger scale variations. Thus a total of 24 simulations were created for each of the 3 models; all of these simulations had random variations in LV position and orientation, normal LV uptake, and extracardiac activity. The means and SDs of these variations are given in Table 1.

Table 1. SD of random variations in simulations

Variable	Mean	SD
LV angular position	–90°, –40°, –45°	5°, 5°, 5°
LV translational position	0, 0, 0	0.5 cm, 0.5 cm, 0.5 cm
LV size (relative)	1.0	0.025 for first 12, 0.05 for second 12
LV counts per pixel	1000	150
Blood pool counts per pixel	100	20
Body counts per pixel	100	20
Liver counts per pixel	500	100
Lung counts per pixel	100	20
Stomach counts per pixel	200	40
Kidney counts per pixel	500	100
Spleen counts per pixel	500	100
Bone counts per pixel	200	20

From each of the resulting 72 NCAT-created activity and attenuation maps, we created simulated projections using a projector that modeled all major degradation factors in SPECT. The projector included a low-energy high-resolution collimator model that incorporated geometric detector response, simulated photon scatter by use of the Klein-Nishina formula, and added standard Poisson-distributed noise according to image count levels, which are noted in Table 1. More details regarding this projector are discussed by Chen et al.[14] Projections were reconstructed via filtered backprojection.

Alignment

Our registration approach operates on processed short-axis slices as a natural intermediate step during perfusion quantification. The automatically selected LV limits of apex, base, long-axis center, and radius of search were used to define the general image area containing the left ventricle. A background region of interest outside and lateral to the LV area was

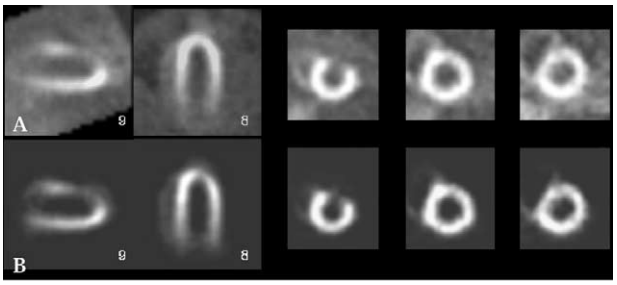

Figure 1. Results of preprocessing a SPECT study before alignment. **A**, Original vertical long-axis, horizontal long-axis, and 3 short-axis slices. **B**, Same slices after background subtraction and elimination of extracardiac objects.

identified automatically by use of these LV limits, and a background subtraction was performed. Then, image counts outside the LV region were rolled off by use of a Gaussian function. In practice, this allowed portions of the right ventricle next to the left ventricle to remain in the processed image. An example of the results of this processing is shown in Figure 1.

The image alignment operation found the best translation, rotation, spatial size, and relative image intensity for one image so that when subtracted from the other image, the difference between them was minimized. The translation, rotation, and spatial size variables account for changes in position and size of the left ventricle between studies. The scaling factor for image intensity accounts for expected differences in absolute count values in different perfusion studies. More specifically, our registration procedure minimized a cost function consisting of the sum of square differences between 2 images over translation, rotation, spatial size, and image intensity. Minimization was performed by use of the Newton-Raphson method to find the roots of the derivative of the cost function, which occur at function minima. This optimization approach is similar to that described in Woods et al,[15] who reported its accuracy in positron emission tomography (PET) brain images. The registration was done in a multiresolution fashion, with the images resampled to one quarter of their original resolution for an initial alignment step, then resampled to one half of their initial resolution for an intermediate alignment step, and then finally registered at their full resolution. We investigated the use of both rigid alignment, which included translations and rotations but no scaling, as well as a full linear alignment, which included translations, rotations, scale, and shear.

Statistical Analysis

Each of the simulations was quantified by use of the Emory Cardiac Toolbox (Syntermed, Atlanta, Ga) before and after rigid and full alignment. LV limits (apex, base, short-axis center, and radius of search) for the original studies were set automatically, with the user adapting them as necessary. In studies that had been aligned, we applied the same LV limits to each of the 2 studies being compared. That is, when we compared study 2 with study 1 after study 2 had been aligned with study 1, we used the original study 1 LV limits for both study 1 and the aligned study 2.

We used a regional approach for detecting perfusion changes based on the quantitative results. First, the intersection of the normal regions, or non–blacked out regions, in the 2 studies was used for intensity normalization of the 2 studies. Study 2 was scaled to have the same average value in the normal region as study 1. Then, the larger of the 2 abnormal regions taken from the 2 studies being compared was used as the region of interest for statistical analysis of changes. The means within this region of interest were compared between the 2 images by use of a paired Student t test.[16] Receiver operating characteristic (ROC) curves were generated by use of these t values—specifically, the difference in means divided by the standard error—to compare the results of rigid, full linear, and original (no alignment) approaches (MedCalc Software, Mariakerke, Belgium). All P values reported in this analysis are 2-tailed, and significance levels are set at $P < .05$.

For each set of 6 perfusion severities, we looked at severity differences of 5%, 10%, and 15%; it should be noted that all perfusion differences in this work are stated in terms of absolute differences (35% to 40% of maximum perfusion is a 5% change). For each set of 12 simulations, we looked at differences where severities were actually the same; these comparisons functioned as "negative" cases for subsequent ROC analysis. These comparisons are shown graphically in Figure 2. We analyzed the first set of 12 simulations in each model (<10% difference in actual LV size changes) separately from the second set of 12 simulations (>10% difference in actual LV size changes). The full set of comparisons done for all 24 simulations in a model is listed in Table 2.

RESULTS

The mean and SDs of the detected changes in abnormally perfused regions are provided in Table 3. In general, detected changes are about half the true differences. Although alignment generally reduces the mean differences, note that it also reduces the SDs. Overall, registration increased t values and detectability of changes. An example of the results of registration, as well as its effect on blackout maps, is shown in Figure 3.

ROC curves for each method are shown in Figure 4, and areas under each are shown in Table 4. For those data sets where the true size of the left ventricle changed by less than 10% between simulations (Figure 4*A-C*), full alignment generally worked better than rigid alignment, which in turn worked better than no alignment (original). Most of the curves are not significantly different from one another, however. Rigid alignment was significantly better than original (no alignment) for detecting 15% and 10% differences in defect severity. Full alignment was significantly better than no alignment for detection of 10% differences in defect severity. Five percent severity differences were not well detected, and neither type of alignment significantly improved results over no alignment.

For those data sets where the true size of the left ventricle changed by more than 10% (Figure 4*D-F*), full

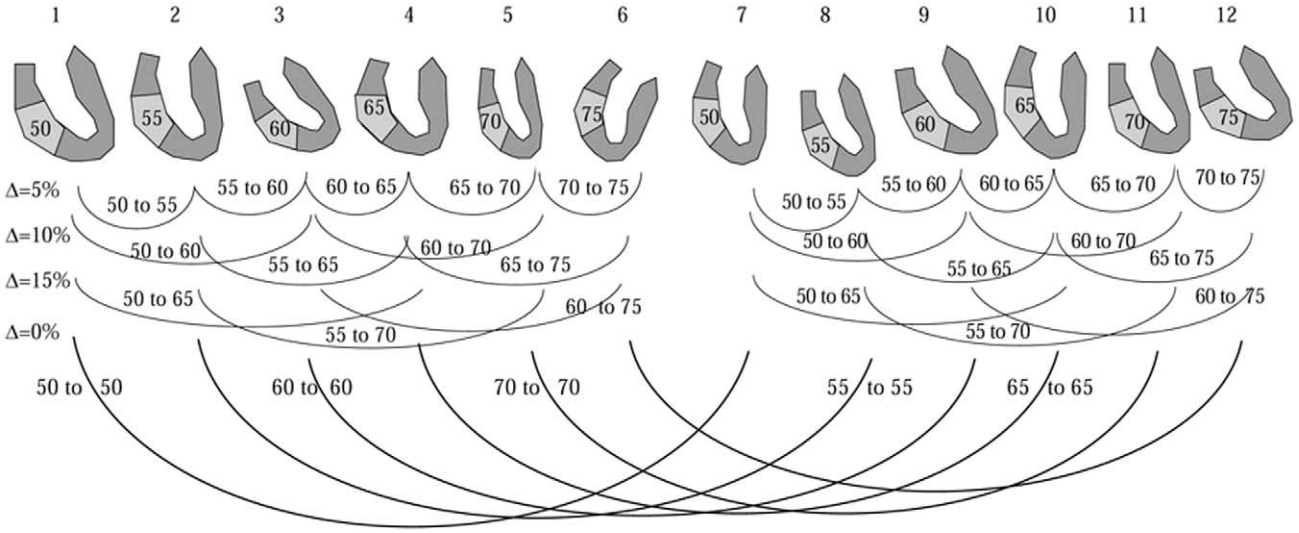

Figure 2. Set of 12 simulations and the comparisons between them. Note from simulation 1 to 6, defect severities (seen in the lighter gray region of the left ventricle) improve by 5% with each successive simulation, where defect severities are expressed in terms of percent of maximum LV perfusion. Simulations 7 to 12 repeat the defect severities of 1 to 6 but may have different positions, sizes, and so on. Note that the differences in LV angle and sizes in this diagram have been somewhat exaggerated for the purpose of demonstration. Comparisons are made between simulations 2 and 1, 3 and 2, and so on; these left ventricles have a 5% difference in severities. Comparisons are made between simulations 3 and 1, 4 and 2, and so on; these left ventricles have a 10% difference in defect severity. Comparisons are made between simulations 4 and 1, 5 and 2, and so on; these left ventricles have a 15% difference in defect severity. Comparisons made between simulations 7 and 1, 8 and 2, and so on, have no (or 0%) difference in defect severity. Note that a second set of 12 simulations with their requisite comparisons is computed for each model; the difference between the 2 sets of 12 is that LV size variations between the simulations are expected to be less than 10% in the first set of 12 and greater than 10% in the second 12.

Table 2. Comparisons performed for 24 simulations created from 1 model

Simulations compared	No. of comparisons	True difference in defect perfusion
1-2, 2-3, 3-4, 4-5, 5-6, 7-8, 8-9, 9-10, 10-11, 11-12	10	5%
1-3, 2-4, 3-5, 4-6, 7-9, 8-10, 9-11, 10-12	8	10%
1-4, 2-5, 3-6, 7-10, 8-11, 9-12	6	15%
1-7, 2-8, 3-9, 4-10, 5-11, 6-12	6	0%
13-14, 14-15, 15-16, 16-17, 17-18, 19-20, 20-21, 21-22, 22-23, 23-24	10	5%
13-15, 14-16, 15-17, 16-18, 19-21, 20-22, 21-23, 22-24	8	10%
13-16, 14-17, 15-18, 19-22, 20-23, 21-24	6	15%
13-19, 14-20, 15-21, 16-22, 17-23, 18-24	6	0%

alignment was always statistically better than original (no alignment). Rigid alignment performed better than no alignment for detecting 10% differences in defect severity, and full alignment performed better than rigid alignment for detecting 5% differences in defect severity. However, once again, 5% severity differences were not well detected even with full alignment, as the area under the ROC curve in this case was only 0.81.

DISCUSSION

The automatic detection of perfusion variations encompasses both image alignment and mathematical comparisons of the matched images. The problem of matching one cardiac SPECT perfusion image to another has been investigated in the realm of aligning stress and rest images of the same patient, matching PET and

Table 3. Average detected differences in defect perfusion

True changes	<10% Scale changes			>10% Scale changes		
	Original	Rigid	Full	Original	Rigid	Full
5%	3.18 ± 5.55*	2.04 ± 3.76*	1.73 ± 3.71	2.85 ± 6.01	2.93 ± 5.24*	2.60 ± 5.24
10%	5.32 ± 5.51*	4.08 ± 3.39*	3.91 ± 4.05*	4.73 ± 6.32*	5.77 ± 5.43*	4.61 ± 5.02*
15%	7.87 ± 5.78*	7.16 ± 4.39*	5.92 ± 4.54*	7.99 ± 6.36*	7.34 ± 5.59*	6.76 ± 5.12*
0%	1.51 ± 5.84	−0.10 ± 3.18	−0.18 ± 3.53	−1.17 ± 7.04	−0.50 ± 5.61	−1.85 ± 6.00

Data are given as mean ± SD.
*The detected differences are significantly different from 0, with $P < .05$.

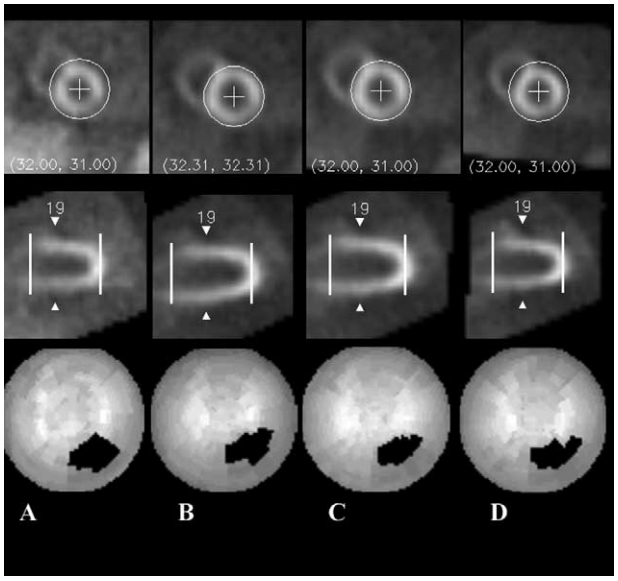

Figure 3. Example of alignment and quantitative results for one of the models. The *top row* and *middle row* show short-axis and vertical long-axis slices, respectively, with LV limits superimposed. The *bottom row* shows the blackout polar maps obtained by perfusion quantification applied to each simulation. **A**, First simulation, with defect severity equal to 55% of normal. **B**, Second simulation with defect severity equal to 65% of normal, which is to be compared with **A**. The difference in size between **A** and **B** is 16%. Here, both left ventricles and **A** and **B** have been reoriented into short-axis slices, but no explicit registration has been performed. The difference between means in the blackout region is less than 1% when **A** is compared with **B**. **C**, Second simulation after rigid alignment. Note that there has been a translation and rotation applied by the registration software. The difference between means in the blackout region is increased to 2% by this alignment. **D**, Second simulation after full linear alignment. Rotation, translation, and scale have been accounted for with this registration. The difference between means in the blackout region is increased to 5%, and this becomes statistically significant with a t value of 5.0.

SPECT images to each other, and even registering dynamic frames of a single patient study. Although none of these approaches was developed for aligning serial studies, they do address an essentially similar problem. Historically, SPECT LV images have been aligned to each other by use of only translation and rotation. In the simplest case this alignment is achieved by finding and aligning the LV long axes in both images.[17,18] More complicated template matching that aligns over translation and rotation of 2 different images has also been described by Slomka et al[19,20] and Turkington et al,[21] for example. The basis of our alignment approach is similar to these; the main differences are the formulation of the cost function that is being minimized and the actual optimization method used to minimize it.

Most reports describing mathematical analysis of perfusion changes rely on evaluation of standard perfusion quantification results. For example, Berman et al[4] looked at differences in summed stress scores to determine perfusion changes in serial studies. Our earlier work indicated that neither summed stress scores nor stress total severity scores were accurate for determining 5% or 10% defect severity changes in single subjects[22]; however, the use of such measures for evaluating a procedure in a large group of patients may have value. deKemp et al[23] have published the description of a method for evaluating perfusion changes in dynamic PET studies. This elegant approach uses changes in absolute quantitated perfusion with a standard error measure evaluated by use of the final frames of the dynamic study to compute t values for every sampled value in the polar map. These can then be used to define significant differences between 2 studies for each polar map value. Unfortunately, in 2 serial SPECT studies of the same patient, we have no way to measure explicitly the standard error for individual polar map samples; thus the method of deKemp et al is not directly applicable. The approach of Slomka et al for finding differences in rest and stress perfusion studies, which includes both registration and normalization for detecting those differences, may be applicable to finding changes in serial studies; however, this use has not yet been described.[20]

We developed this approach—that is, computing

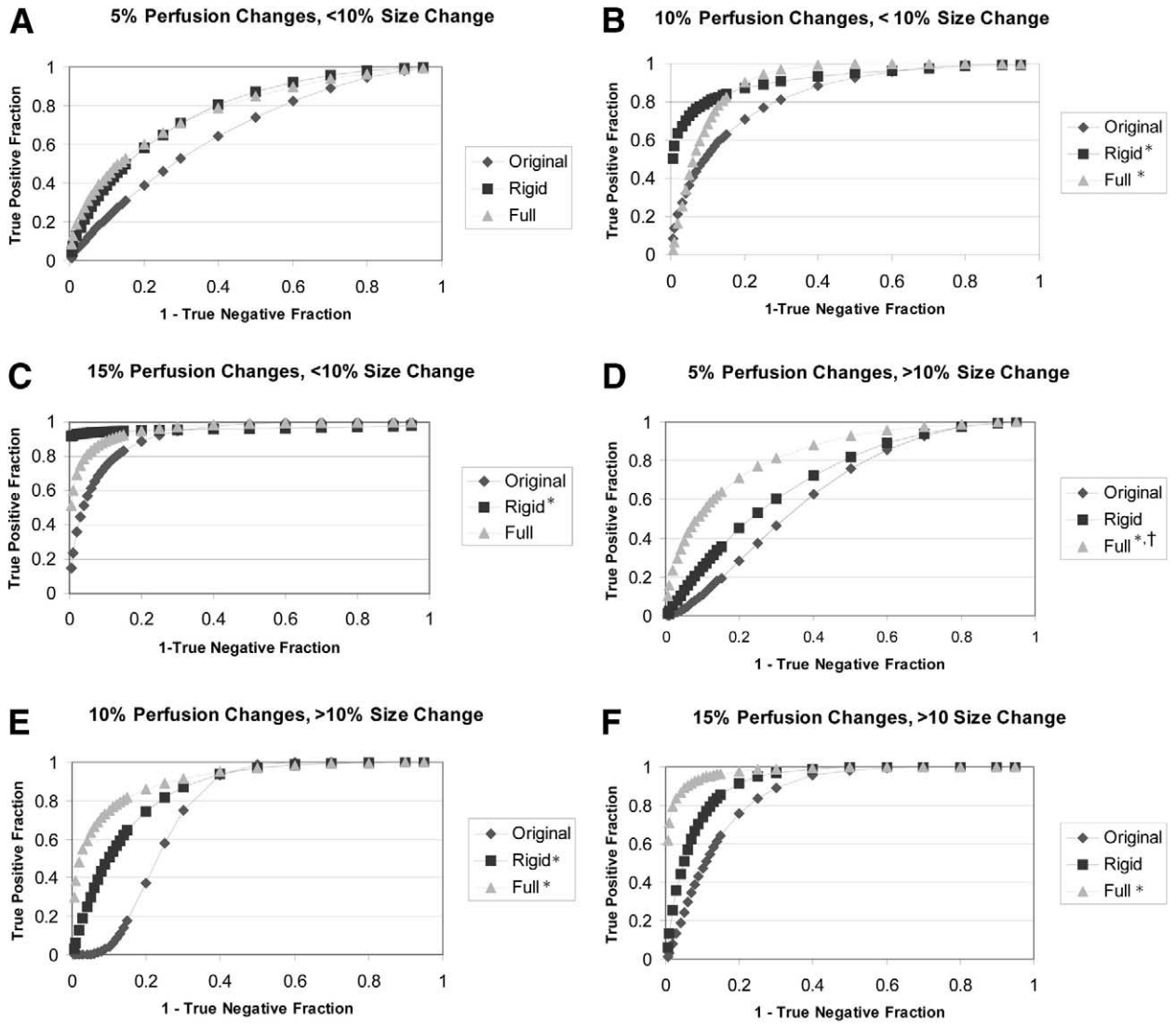

Figure 4. ROC curves for the 3 types of alignment (none, rigid, and full linear) for each comparison (5%, 10%, and 15% differences in defect severity). Curves are given separately for the cases where LV scale changes by both less (**A**, **B**, and **C**) and more than 10% (**D**, **E**, and **F**). The *asterisk* indicates that the area under this curve is significantly different from the area under the "original," or unaligned, curve within the same column ($P < .05$). The *dagger* indicates that the area under this curve is significantly different from the area under the "rigid" curve within the same column ($P < .05$).

Table 4. Area under ROC curves associated with perfusion changes

Alignment type	LV size differences <10%			LV size differences >10%		
	5%	10%	15%	5%	10%	15%
Original	0.67	0.81	0.91	0.67	0.76	0.83
Rigid	0.74	0.91*	0.99*	0.71	0.84*	0.92
Full	0.75	0.93*	0.96	0.81*†	0.91*	0.98*

*The area under this curve is significantly different from the area under the "original," or unaligned, curve within the same column.
†The area under this curve is significantly different from the area under the "rigid" curve within the same column.

statistically significant differences within defects—partially because such regional analysis provides a straightforward way for the standard error to be estimated from only 2 serial studies of the same patient. In addition, it was the most accurate method among various techniques we investigated in preliminary studies.[22] Unfortunately, it is obviously limited to those regions that are abnormal and does not attempt to say anything about other regions of the left ventricle. However, because most patients who undergo serial studies do so because they have perfusion abnormalities, this is not a serious limitation in the clinical setting. Also, it would of course be possible to define other regions of interest in the left ventricle that were not based on blackout areas.

None of the registration approaches in this study allowed a reliable detection of 5% differences in perfusion for single patients. This is not unexpected, given that maximum true LV count levels in these simulations were on the order of 1000 and reconstructed images had mean LV counts per pixel of approximately 600. The noise rate of the Poisson-distributed counts in such an image is about 4%, and this raises the standard error enough that t values do not reach significant levels with a perfusion severity difference of only 5%. Fifteen percent differences in perfusion defect severity were fairly well detected even with no alignment when LV scale changes were minimal. This result may seem surprising; however, reformatting transverse slices into short-axis sections is a type of alignment performed before quantification, and resampling the left ventricle to create polar maps actually standardizes the left ventricles in terms of scale. Thus standard perfusion quantification already includes some implicit alignment. Explicit registration of the short-axis slices improves upon that, however, and our results indicate that full registration is advisable for automatic detection of even 15% perfusion differences when LV sizes change by more than 10% between serial studies.

Detected differences are lower than the true differences primarily because of detector response. Just as the severity and extent of a defect are underestimated as a result of the inherent blurring of SPECT, the severity of perfusion changes may also be underestimated. This effect is magnified in our analysis because we are reporting mean differences over the perfusion defect, which of course will encompass regions close to the margins of the abnormality. The difference between maximal perfusion values in the defect would be closer to the true value; however, use of maximum regional values instead of mean values would preclude the utilization of parametric models for statistical analysis. Also, note that Table 3 indicates that detected perfusion differences actually decrease with registration. This is simply explained by considering that differences between 2 studies are a result of both misregistration and perfusion changes. The registration method operates by trying to minimize differences between the images; thus registration will also diminish differences between perfusion defect severities in 2 studies if those defects were affected by misalignment. However, it is just as important to note that registration generally decreases the SDs of those differences. A reduced SD increases t values and, thus, detectability of perfusion changes. In fact, mean group t values were always higher for rigid versus no registration and were higher again for full registration for cases where the LV size varied by more than 10%. This is reflected in the ROC curves. For cases where the LV size changed by less than 10%, mean t values increased with full registration compared with no registration but were generally higher with rigid registration than with full registration. This is clearly visible on the ROC curves; however, the difference was not significant.

Although these simulation results appear to indicate that our approach cannot detect 5% changes in defect severity, this is not so. Changes in defect severity smaller than 10% may be detected in groups of subjects. The means and SDs obtained in each comparison can be used to estimate roughly the number of patients necessary to achieve significance for detecting 5% and 10% severity changes. Without registration, approximately 50 patients may be needed to detect a 5% change in defect severity with $P < .05$ and approximately 10 patients may be needed to detect a 10% change in defect severity. If alignment is used, this is reduced to approximately 20 patients to detect a 5% change in defect severity and 5 patients to detect a 10% change in defect severity ($P < .05$). Of course, these are rough guidelines; for studies interested in evaluating smaller or less severe defects than the ones considered in this study, larger groups might be necessary. For studies evaluating changes in larger or more severe defects, a smaller group might be sufficient. Findings such as these should have a profound implication for clinical trials that use perfusion changes as endpoints by significantly reducing the numbers of subjects needed and thus the trial duration and cost.

Of course, in a common clinical setting, it is more important to be able to detect perfusion differences reliably in a single patient. Our approach for finding perfusion changes can be evaluated by use of the ROC curves. They indicate that when studies are fully aligned, this method can detect a 10% change in defect severity in a single patient with a false-positive rate of 15% while maintaining a true-positive fraction of near 90%. A change of 15% in defect severity can be detected with a false-positive rate of 10% while maintaining a true-positive fraction of over 90%.

In this study we always compared higher (more normal) with lower perfusion, so statistically significant

t values should be positive, indicating a significant improvement in perfusion. However, this study would have yielded the exact same results if we had looked at the accuracy of the method for detecting significant decreases in perfusion, as the mathematics would have simply changed in sign value. However, there is a difference in how these results are handled statistically versus how they would be handled clinically, and this is worth noting. Consider the case of obtaining a highly negative t value (eg, $t < -2.5$) indicating that perfusion may have worsened in the case where perfusion in fact improved. This would be seen as a false negative by our statistical analysis, just as if the t value had been zero, indicating no change. Clinically, however, a statistical indication of significantly decreasing perfusion would be handled much differently than a statistical indication of no change. Our method resulted in statistically significant decreases in perfusion ($t < -2.5$) in about 15% of cases where perfusion actually increased by 5%, and alignment did not improve these results. We saw only 1 case where our technique indicated a significant decrease in perfusion severity when there was actually a 10% increase in severity, and alignment eliminated this single instance. We saw no negative t values at all for true defect severity increases of 15%.

Although we believe that these numbers provide an indication of the ability of SPECT imaging to detect perfusion changes, it is important to understand the relatively low numbers of simulations investigated in this study, as well as the limited changes applied to them. Real patient data may change in more significant ways than our simulations. The body habitus may change drastically, cardiac remodeling may occur, or camera hardware may be completely different between studies. Perfusion in regions of the heart not previously seen as abnormal may change; this may affect the alignment as well as the normalization performed before t value calculations.

Nevertheless, our simulation was much more realistic that simply applying linear transforms to the reconstructed images and then attempting to recover those transforms with a registration algorithm. The translation, rotation, and scale were applied to the LV model within the NCAT torso, and LV counts and extracardiac activity were varied before simulation of the acquisition process. This implies that in different simulations, the heart may in fact experience different attenuation, scatter, and detector response, and thus local LV counts will vary even in "normal" regions of the heart. These will all confound the alignment algorithm, which is attempting to reduce differences between the images. Even with these complicating factors, it was possible to register, normalize, and compare SPECT perfusion studies with enough accuracy to detect 10% or larger changes in defect severity for single patients.

Conclusion

The following clinically relevant points may be concluded from this study. True differences in perfusion are larger than those measured by perfusion SPECT by an approximate factor of 2. Differences in defect severity of 10% and 15% may be detected in serial perfusion studies of a single patient by our method with false-positive rates of 15% and 10%, respectively, when full alignment is used. Automatic methods may fail to detect perfusion differences of 5% in serial studies of a single patient; however, groups of patients may be used to detect small perfusion differences in populations for the purpose of therapy evaluation. Alignment reduces the number of studies necessary to demonstrate a significant perfusion change in groups of patients by about half.

Acknowledgment

The authors have indicated they have no financial conflicts of interest.

References

1. Losordo DW, Vale PR, Symes JF, Dunnington CH, Esakof DD, Maysky M, et al. Gene therapy for myocardial angiogenesis: initial clinical results with direct myocardial injection of phVEGF165 as sole therapy for myocardial ischemia. Circulation 1998;98:2800-4.
2. Neglia D, Sambuceti G, Giorgetti A, Bartoli M, Salvadori P, Sorace O, et al. Effects of long-term treatment with verapamil on left ventricular function and myocardial blood flow in patients with dilated cardiomyopathy without overt heart failure. J Cardiovasc Pharmacol 2000;36:744-50.
3. Van Belle E, Abolmaali K, Bauters C, McFadden EP, Lablanche JM, Bertrand ME. Restenosis, late vessel occlusion and left ventricular function six months after balloon angioplasty in diabetic patients. J Am Coll Cardiol 1999;34:476-85.
4. Berman DS, Kang X, Schisterman EF, Gerlach J, Kavanagh PB, Areeda JS, et al. Serial changes on quantitative myocardial perfusion SPECT in patients undergoing revascularization or conservative therapy. J Nucl Cardiol 2001;8:428-37.
5. Dakik HA, Kleiman NS, Farmer JA, He ZX, Wendt JA, Pratt CM, et al. Intensive medical therapy versus coronary angioplasty for suppression of myocardial ischemia in survivors of acute myocardial infarction: a prospective, randomized pilot study. Circulation 1998;98:2017-23.
6. Lind PA, Pagnanelli R, Marks LB, Borges-Neto S, Hu C, Zhou SM, et al. Myocardial perfusion changes in patients irradiated for left-sided breast cancer and correlation with coronary artery distribution. Int J Radiat Oncol Biol Phys 2003;55:914-20.
7. Schmitt C, Meyer C, Kosa I, Weyerbrock S, Schneider M, Zrenner B, et al. Does radiofrequency catheter ablation induce a deterioration in sympathetic innervation? A positron emission tomography study. Pacing Clin Electrophysiol 1998;21:327-30.

8. Wackers RJTh. Science, art and artifacts: how important is quantification for the practicing physician interpreting myocardial perfusion studies? J Nucl Cardiol 1994;1:s109-17.
9. Garcia EV, Van Train K, Maddahi J. Quantification of rotational thallium-201 myocardial tomography. J Nucl Med 1985; 26:17-26.
10. Garcia EV, Cooke CD, Van Train KF, Folks R, Peifer J, DePuey EG, et al. Technical aspects of myocardial SPECT imaging with Tc-99m sestamibi. Am J Cardiol 1990;66:23E-31E.
11. Terry JA, Tsui BMW, Perry JR, Hendricks JL, Gullberg GT. The design of a mathematical phantom of the upper human torso for use in 3-D SPECT imaging research. In: Mikulecky DC, Clarke AM, editors. Biomedical engineering: opening new doors. New York: New York University Press; 1990. p. 185-90.
12. Segars WP, Lalush DS, Tsui BMW. A realistic spline-based dynamic heart phantom. IEEE Trans Nucl Sci 1999;46:503-6.
13. Faber TL, Garcia EV, Lalush DS, et al. Simulating patient-specific heart shape and motion using SPECT perfusion images with the NCAT phantom. In: Mun SK, editor. Visualization, display, and image guided procedures. Bellingham, Wash: SPIE 4319. 2001. p. 22-6.
14. Chen J, Galt JR, Valentine JD, Faber TL, Garcia EV. Modelling SPECT acquisition and processing of changing radiopharmaceutical distribution. Nuclear Science Symposium and Medical Imaging Conference. Piscataway, NJ: IEEE Press. p. 1336-70.
15. Woods RP, Cherry SR, Mazziotta JC. Rapid automated algorithm for aligning and reslicing PET images. J Comput Assist Tomogr 1992;16:620-33.
16. Neter J, Kutner MH, Nachtsheim CJ, Wasserman W. Applied linear statistical models. Chicago: Richard D. Irwin, Inc; 1996. p. 3-94.
17. Germano G, Kavanagh PB, Su HT, Mazzanti M, Kiat H, Hachamovitch R, et al. Automatic reorientation of 3-dimensional transaxial myocardial perfusion SPECT images. J Nucl Med 1995;36:1107-14.
18. Mullick R, Ezquerra NF. Automatic determination of left ventricular orientation from SPECT data. IEEE Trans Med Imaging 1995;14:88-99.
19. Slomka PJ, Hurwith GA, Stephenson J, Cradduck T. Automated alignment and sizing of myocardial stress and rest scans to three-dimensional normal templates using an image registration algorithm. J Nucl Med 1996;36:1115-22.
20. Slomka PJ, Nishina H, Berman DS, Kang X, Friedman JD, Hayes SW, et al. Automatic quantification of myocardial perfusion stress-rest change: a new measure of ischemia. J Nucl Med 2004;45:183-91.
21. Turkington TG, DeGrado TR, Hanson MW, Coleman RE. Alignment of dynamic cardiac PET images for correction of motion. IEEE Trans Nucl Sci 1997;44:235-42.
22. Faber TL, Galt JR, Chen J, Tsui BMW, Garcia EV. Detecting changes in myocardial perfusion. In: Lemke HU, Vannier MW, Inamura K, Forman AG, Doi K, Reiber JHC, editors. Computer-assisted radiology and surgery. Berlin: Springer-Verlag; 2002. p. 879-83.
23. deKemp RA, Ruddy TD, Hewitt T, Dalipaj MM, Beanlands RS. Detection of serial changes in absolute myocardial perfusion with Rb-82 PET. J Nucl Med 2000;41:1426-35.